Pergamon

Int. J. Heat Mass Transfer. Vol. 38, No. 15, pp. 2843–2854, 1995

0017-9310/95 $9.50+0.00

0017-9310(95)00002-X

Numerical modeling of ablation phenomena as two-phase Stefan problems

M. STORTI

Grupo de Tecnología Mecánica del INTEC, Universidad Nacional del Litoral and CONICET, Güemes 3450, 3000-Santa Fe, Argentina

(*Received* 4 *January* 1994 *and in final form* 21 *November* 1994)

Abstract—A fixed domain numerical scheme for ablation problems based on the enthalpy formulation and with temperature as the main dependent variable is presented. A fictitious material which occupies the region where the material has been removed is introduced, and its material properties are: null specific heat and any value for the conductivity, preferably that of the lower temperature phase. The ablating surface is transformed on an internal interface and the thermal load there is represented as a concentrated internal heat source on the interface. The resulting two-phase Stefan problem is discretized with the scheme presented in a series of previous papers. Finally, several numerical examples are presented.

1. INTRODUCTION

Thermal ablation is a very important problem in aerospace industry [1–6] (thermal protection of space vehicles during the re-entry stage and in rocket nozzles) and laser welding. A severe heat flux, typically coming from radiation or convection, is applied to the body, which is initially in 'virgin' phase. As the temperature rises, it can experience one or several chemical transformations. In the case of thermal protection for the aerospace industry these are, typically, pyrolysis with gas emission and melting. For the thermal protection to be effective all these reactions must be strongly endothermic. The material exposed to the thermal load is removed by several effects: mechanical (high shear stresses in the aerodynamic boundary layer) or chemical. In the case of a phase-change to a phase with very low mechanical strength, the material is removed immediately after it reaches the phase-change temperature. This is the Stefan-type or phase-change ablation and it will be the physical model adopted in what follows.

Ablation problems, as well as one or two-phase Stefan problems, are *moving boundary problems*, and the simplest approach to their numerical solution is some kind of adaptative moving mesh. However, for the two-phase Stefan problem, the so called *enthalpy formulation* circumvents the problem by introducing a single *enthalpy balance equation* which can be solved on fixed meshes [7–10]. The phase-change is present as a singularity in the enthalpy–temperature relationship and the interface is 'captured' by the algorithm, rather than being 'tracked'. In a series of papers we presented a discretization scheme based on the enthalpy formulation for two (or more) phase Stefan problems. The scheme has the temperature as the main unknown and is based on a straightforward Galerkin weighted-residual formulation of the enthalpy balance equation. Moreover it has no regularization parameters. Key points of the method are: the accurate integration of a discontinuous quantity, namely the enthalpy, over the partially melted elements [11] and the efficient solution of the nonlinear resulting system, described in [12].

The basic idea of the present work is to put the one-phase ablation problem in the context of the two-phase Stefan one by means of the introduction of a fictitious phase occupying the region where the material has been removed. This fictitious phase exists at temperatures above the phase-change one and it has null specific heat so that eventual variations of temperature do not contribute to the energy balance. Furthermore, its conductivity is specified as the same of the low temperature phase, so that its thermal diffusivity is infinitely higher than that of the low temperature phase. As a consequence, the fictitious phase is always in a quasi-steady state and, due to the particular boundary condition (null flux at initial boundaries and temperature equal to the melting one at the interface), it has a uniform temperature infinitesimally higher than the melting one.

2. PROBLEM DESCRIPTION

For simplicity we will assume no intermediate transformation so that, as the virgin material is heated and its temperature exceeds the melting temperature T_m, it changes into the low mechanical strength phase and is instantaneously removed. Initially, the virgin material occupies the domain Ω with boundary Γ. Due to thermal loads $\bar{q}$ over certain part of the boundary $\Gamma_q(t=0) \subset \Gamma$, the temperature rises and once the T_m is reached at some time $t = t_0$ at some point of the boundary, the material begins to be removed. For $t > t_0$ we have the domain Ω partitioned in two:

NOMENCLATURE

c_p	specific heat
D	thermal diffusivity
$\mathrm{erf}(x)$	error function
f	scaled temperature profile
$\mathbf{f}$	vector of conductive fluxes
$\mathbf{g}$	vector of thermal loads
$h(T)$	enthalpy
$\mathbf{h}$	vector of nodal enthalpies
k	thermal conductivity
l	characteristic decay length of the temperature profile (see Section 5.2)
L	latent heat
$()^L$	term coming from the latent heat contribution to the enthalpy
$\mathbf{M}^L$	interface capacity matrix
$\hat{\mathbf{n}}$	unit normal
N_μ	FEM-interpolation function
p, q	integer numbers
Q	volume heat source
$\bar{q}$	thermal load at the boundary
$()_{rem}$	refers to the removed zone
$s, \dot{s}$	ablating surface position in one-dimensional problems, recession rate for 1D problems
dS	elementary portion of the interface
s_0	initial position of the interface (see Section 5.1)
s^n	position of the interface for the FEM method at time t^n
Ste	Stefan number
t	time
t_0	preheating time
Δt	time step
Δt^*	non-dimensional time step for the constant load problem
T	temperature
T_i	initial temperature field
T_m	melting temperature
$\bar{T}$	prescribed temperature on the Dirichlet boundary
T_{fic}	temperature in the fictitious phase
$\mathbf{T}$	vector of nodal temperatures
v	recession rate of the ablating surface
v_∞	limit recession rate
x	one-dimensional coordinate
$\mathbf{x}$	vector of spatial coordinates.

Greek and mathematical symbols

α	temporal discretization parameter
ϕ	test function
Γ	boundary
Γ_m	interface
θ	(1) incidence angle in the definition of the fluxes (2) non-dimensional temperature in the transition zone
$\Gamma_q(t)$	boundary of $\Omega_v(t)$ where thermal loads are applied
Γ_T	Dirichlet part of the boundary
λ	correction factor for the characteristic length of the 1D constant-load problem
μ	non-dimensional spatial coordinate in the transition region
ρ	density
τ	characteristic decay time
Ω	domain of resolution
$\emptyset$	empty set.

Subscripts and superscripts

fic	fictitious material
L	part of the enthalpy coming from the latent heat
rem	region where material has been removed
v	virgin material
n	time level t^n
μ, ν	node indices for FEM.

$\Omega = \Omega_v(t) \cup \Omega_{rem}(t)$ (from 'virgin' and 'removed', see figure). Due to the removal of some part of the material, the surface exposed to the thermal load is no longer $\Gamma_q(t=0)$, but it is composed by part of it and the moving boundary. If the thermal load is no longer applied after a certain moment, the temperature of the moving boundary could descend below T_m and the front ceases to advance.

All this cases are included in the following governing equations:

given $T_i(\mathbf{x})$ for $\mathbf{x}$ in Ω, $\bar{q}(t, T(\mathbf{x}), \mathbf{x})$ for $t > 0$ and $\mathbf{x}$ in $\Gamma_q(\mathbf{t})$, and $\bar{T}(\mathbf{x}) < T_m$ for $\mathbf{x}$ in Γ_T, find $\Omega_v(t)$ and $T(\mathbf{x}, t)$ for $t > 0$ and $\mathbf{x} \in \Omega_v(t)$ such that:

$$\rho c_p \dot{T} = \nabla \cdot (k \nabla T) \quad \mathbf{x} \in \Omega_v(t), t > 0 \tag{1}$$

$$Lv - k \left.\frac{\partial T}{\partial n}\right|_{\Gamma_q(t)} = \bar{q}(T|_{\Gamma_q}) \quad \text{on } \Gamma_q(t) \tag{2}$$

$$T = \bar{T} \quad \text{on } \Gamma_T \tag{3}$$

$$\partial\Omega_v = \Gamma_q(t) \cup \Gamma_T \tag{4}$$

where v is the recession rate in the normal direction to the ablating surface and is restricted by the following complementary conditions:

$$T < T_m \quad v = 0 \quad \text{(stationary front)} \tag{5}$$

$$T = T_m \quad v \geqslant 0 \quad \text{(moving front)} \tag{6}$$

and initial conditions:

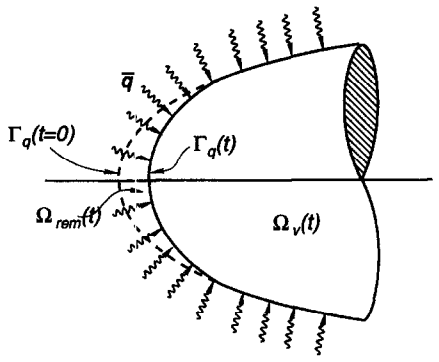

Fig. 1. Description of a typical ablation problem.

$$T(\mathbf{x},0) = T_i(\mathbf{x}) \quad \mathbf{x}\in\Omega \tag{7}$$

$$\Omega_v(t=0) = \Omega \quad \Omega_{rem}(t=0) = \emptyset. \tag{8}$$

Here k is the thermal conductivity, and L the latent heat of the phase change. Equation (2) is the usual energy balance at the interface for moving boundary problems. The expression for $\bar{q}$ is often more complicated, since, in general, it involves a boundary layer calculation over the surface of the body and, then, results in a non-local function, depending on the global shape of the ablating surface $\Gamma_q(t)$. However, this complex dependence is treated in an explicit form and, then, the presented representation is quite sufficient to explain the algorithm.

3. TWO-PHASE EQUIVALENT FORMULATION

3.1. *Two-phase formulation for the 1D problem*

For the one-dimensional (1D) semi-infinite problem equations (1)–(8) reduce to:

given $T_i(x)$ for $x > 0$ and $\bar{q}(t)$ for $t > 0$, find $s(t)$ for $t > 0$ and $T(x,t)$ for $t > 0$, $x > s(t)$ such that:

$$\rho c_p \dot{T} = k\frac{\partial^2 T}{\partial x^2} \quad x > s(t) \quad t > 0 \tag{9}$$

with boundary conditions:

$$-k\frac{\partial T}{\partial x} + L\dot{s} = \bar{q}(t) \quad \text{on } x = s(t) \tag{10}$$

$$T(s(t)) = T_m \text{ and } \dot{s} > 0 \quad \text{or} \quad T(s(t)) < T_m \text{ and } \dot{s} = 0 \tag{11}$$

and initial conditions:

$$s(0) = 0 \quad T(x,0) = T_i(x). \tag{12}$$

For simplicity suppose k, ρc_p constants and $\bar{q}$ depending only on time, i.e. not on surface temperature as in the case of radiation or convection. A possible extension to a two-phase Stefan problem is the following: the fictitious phase exists for $T > T_m$ and $k_{fic} = k_v$, $\rho c_{p_{fic}} = 0$. The thermal load $\bar{q}(t)$ is applied on $x = 0$ (see Fig. 2). In detail:

given $T_i(x)$ for $x > 0$ and $\bar{q}(t)$ for $t > 0$, find $T(x,t)$ such that for $x > 0, t > 0$:

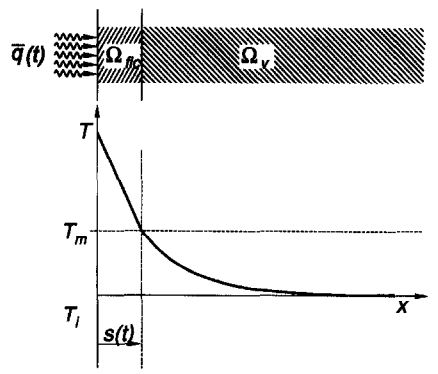

Fig. 2. Two-phase formulation of the one-dimensional problem. First version : the thermal load is applied at the surface and is transmitted without inertia through the fictitious material.

$$\dot{h} = \frac{\partial}{\partial x}\left(k(T)\frac{\partial T}{\partial x}\right) \tag{13}$$

with boundary conditions:

$$-k\frac{\partial T}{\partial x} = \bar{q}(t) \quad \text{on } x = 0, t > 0 \tag{14}$$

and initial conditions:

$$T(x,0) = T_i(x) \quad \text{para } t = 0. \tag{15}$$

The enthalpy function is [see Fig. 3 for the general case $c_{p_v} = c_{p_v}(T)$]:

$$h(T) = \begin{cases} \rho c_{p_v}(T - T_m); & T < T_m \\ L; & T \geqslant T_m \end{cases} \tag{16}$$

($h(T_m^-) = 0$ has been taken as the reference enthalpy).

In what follows, we will show how this formulation reduces to the original one, equations (9)–(12). The non-trivial part of the demonstration consists in showing how the energy balance at the interface (10) is enforced for $t > t_0$. The specific heat is null in the fictitious phase $0 \leqslant x \leqslant s(t)$ so that it is in a steady state:

$$\frac{\partial}{\partial x}\left(k\frac{\partial T}{\partial x}\right) = 0 \quad \text{in } 0 \leqslant x < s(t) \tag{17}$$

then:

$$-k\frac{\partial T}{\partial x}\bigg|_{s(t)^-} = -k\frac{\partial T}{\partial x}\bigg|_0 = \bar{q}(t) \tag{18}$$

but, by the energy balance at the interface for the two-phase problem:

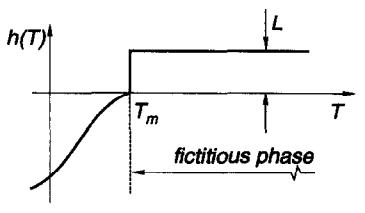

Fig. 3. Enthalpy function for the two-phase formulation.

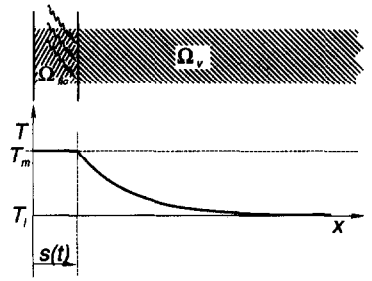

Fig. 4. Two-phase formulation of the one-dimensional problem. Second version : the thermal load is added as a heat source strongly localized at the interphase. Temperature in the fictitious phase is constant and equal to T_m^+.

$$-k\frac{\partial T}{\partial x}\bigg|_{s(t)^+} + k\frac{\partial T}{\partial x}\bigg|_{s(t)^-} = L\dot{s} \quad t > t_0. \tag{19}$$

From (18) and (19) we obtain the desired energy balance at the surface:

$$-k\frac{\partial T}{\partial x}\bigg|_{s(t)^+} + L\dot{s} = \bar{q}(t). \tag{20}$$

This formulation is very well suited to apply all the theory from the two-phase problem (the resulting system is symmetric and positive definite). However it can not be extended to the multidimensional case: in 1D all the heat flux imposed at $x = 0$ is transmitted to the free boundary trough the fictitious phase without inertia. In the multidimensional case the heat flux applied at the original surface of the body is redistributed in the fictitious phase and there is no control on the flux density at each point of the interface. However, a good approximation can be obtained with this formulation if the variation of the flux on the surface is smooth and the curvature small.

To overcome this difficulty for the general case, the formulation is slightly modified as follows: the thermal load $\bar{q}$ is no longer applied at $x = 0$ but is represented as a concentrated heat source in the interface (see Fig. 4). The properties for the fictitious phase are the same as in the previous model:

given $T_i(x)$ for $x > 0$ and $\bar{q}(t)$ for $t > 0$, find $T(x, t)$ for $t > 0$, $x > 0$ such that:

$$\dot{h} = \frac{\partial}{\partial x}\left(k(T)\frac{\partial T}{\partial x}\right) + Q(x,t) \quad \text{in } x > 0 \tag{21}$$

with boundary conditions:

$$-k\frac{\partial T}{\partial x} = \begin{cases} \bar{q}(t) & \text{if } T(x=0,t) < T_m \\ 0 & \text{if } T(x=0,t) \geqslant T_m \end{cases} \quad \text{at } x = 0 \tag{22}$$

and initial conditions:

$$T(x,0) = T_i(x). \tag{23}$$

The heat source $Q(x, t)$ is proportional to a Dirac's δ distribution at the moving front $T = T_m$, with a total amount of heat delivered per unit time given by the thermal load $\bar{q}(t)$:

$$\int_0^\infty Q(x,t)\phi(x)\,dx = \bar{q}(t)\phi(s(t)) \tag{24}$$

for every smooth but otherwise arbitrary test function ϕ. Now, we will show how this formulation is equivalent to the original one. As in the previous formulation, the fictitious phase is in the steady state and, then, the heat flux is constant throughout:

$$-k\frac{\partial T}{\partial x}\bigg|_{s(t)^-} = -k\frac{\partial T}{\partial x}\bigg|_0 = 0. \tag{25}$$

The energy balance at the interface, taking account of the concentrated source Q, is:

$$-k\frac{\partial T}{\partial x}\bigg|_{s(t)^-} = -k\frac{\partial T}{\partial x}\bigg|_{s(t)^+} + L\dot{s} - \int_{s(t)^-}^{s(t)^+} Q(x,t)\,dx \tag{26}$$

Now, using equations (24) and (25):

$$-k\frac{\partial T}{\partial x}\bigg|_v + L\dot{s} = \bar{q}(t) \tag{27}$$

and the desired energy balance is enforced.

3.2. *The multidimensional problem*

The extension to the multidimensional case is now obvious:

given $T_i(\mathbf{x})$ for x in Ω, $\bar{q}(t, \mathbf{x}, T(\mathbf{x}))$ for $t > 0$ and $\mathbf{x}$ in Ω, find $T(\mathbf{x}, t)$ for $\mathbf{x}$ in Ω, $t > 0$ such that:

$$\dot{h} = \nabla\cdot(k\nabla T) + Q(\mathbf{x},t) \quad \text{in } \Omega, t > 0 \tag{28}$$

with boundary conditions:

$$k\frac{\partial T}{\partial n} = \begin{cases} \bar{q}(t); & \text{if } T < T_m \\ 0; & \text{if } T \geqslant T_m \end{cases} \text{in } \Gamma_q (t = 0) \tag{29}$$

$$T = \bar{T} \quad \text{in } \Gamma_T \tag{30}$$

where Ω_{rem} has been replaced by Ω_{fic}, $\hat{\mathbf{n}}$ is the unit normal exterior to Ω_{fic}, and initial conditions:

$$T(\mathbf{x},0) = T_i(\mathbf{x}) \quad \text{for } t = 0 \tag{31}$$

$h(T)$ is defined always by (16) and the generalization of the definition of Q (24) is:

$$\int_\Omega Q(\mathbf{x},t)\phi(\mathbf{x})\,d\Omega = \int_{\Gamma_m} \bar{q}(\mathbf{x})\phi(\mathbf{x})\,dS. \tag{32}$$

To show the equivalence to the original ablation problem, equations (1)–(8), we note first that, as the specific heat of the fictitious phase is null, we have:

$$\nabla\cdot(k\nabla T) = 0 \quad \text{in } \Omega_{fic} \tag{33}$$

with boundary conditions

$$-k\frac{\partial T}{\partial n} = 0 \quad \text{in } \Gamma_q (t = 0) \quad \text{and}$$

$$T = T_m \quad \text{in } \Gamma_m \text{ (moving front)}. \tag{34}$$

The solution to this steady problem is trivial:

$$T \equiv T_m \quad \text{in } \Omega_{fic}. \tag{35}$$

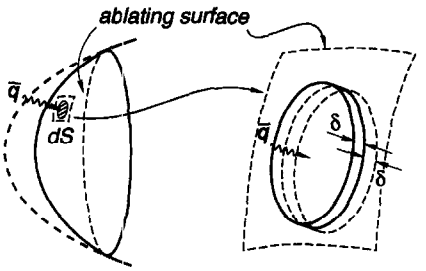

Fig. 5. Control volume enclosing an elementary portion of the ablating surface.

But this implies that the heat flux coming to the interface from the fictitious phase is null:

$$-k\frac{\partial T}{\partial n}\bigg|_{\text{fic}} = 0. \tag{36}$$

Writing down an energy balance over a thin cylindrical control-volume of thickness δ enclosing an elementary portion of surface dS of the ablating surface (see Fig. 5), we have that:

$$-k\frac{\partial T}{\partial n}\bigg|_{\text{fic}} dS + k\frac{\partial T}{\partial n}\bigg|_{\text{v}} dS + Q\,dS\,\delta = Lv_{\text{n}}\,dS \tag{37}$$

where $\hat{\mathbf{n}}$ is the unit normal exterior to Ω_{fic}. But, from the definition of Q, equation (32):

$$Q\,d\Omega = Q\,dS\,\delta = \bar{q}\,dS \tag{38}$$

replacing equations (38) and (36) in (37) we arrive at the desired energy balance at the interface:

$$-k\frac{\partial T}{\partial n}\bigg|_{\text{v}} + Lv_{\text{n}} = \bar{q} \quad \text{in}\,\Gamma_{\text{m}}. \tag{39}$$

Regarding the extension to non-isothermal ablation problems, i.e. when the ablation temperature is determined by an additional balance relationship, the key point is that the solution to equations (33) and (34) with a T_{m} depending on position is no longer a constant temperature field and, then, equation (36) is false. This problem can be solved by setting the conductivity to a very low value in order to eliminate conduction through the fictitious phase. However, this extension has not been implemented so far.

4. DISCRETIZATION SCHEME

Once the ablation problem has been cast in the form of an equivalent two-phase Stefan problem, any discretization scheme for this last, simpler, problem can be applied. Certainly, the equivalent two-phase problem is harder than typical two-phase Stefan problems due to the null specific heat for the fictitious phase, and some degree of robustness of the scheme is advisable. In what follows we will briefly review the discretization scheme which has been presented in previous papers [11, 12], and has been used successfully in the numerical experiments presented in Section 5.

First we recall the variational formulation of the Stefan problem:

$$\frac{d}{dt}\int_\Omega \phi h\,d\Omega + \int_\Omega \nabla\phi\cdot k\nabla T\,d\Omega - \int_{\Gamma_q}\phi\bar{q}\,dS - \int_\Omega \phi Q\,d\Omega = 0 \tag{40}$$

where ϕ is a test function in such a way that it vanishes at the Dirichlet boundary. As usual in the finite element method (FEM) the temperature field is approximated by:

$$T(\mathbf{x},t) = \sum_{\mu=1}^{N} T_\mu(t)N_\mu(\mathbf{x}) \tag{41}$$

where μ is a node index and the $\{N_\mu(\mathbf{x})\}$ are FEM interpolation functions. Also, the interpolation functions corresponding to those nodes which do not belong to the Dirichlet part of the boundary are taken as test functions. Replacing equation (41) in (40) and ϕ by each of the interpolation functions we obtain a nonlinear ODE's system of the form:

$$\frac{d}{dt}\{\mathbf{h}(\mathbf{T})\} = \mathbf{f}(\mathbf{T}) + \mathbf{g}(t) \tag{42}$$

where $\mathbf{h}$, $\mathbf{f}$ and $\mathbf{g}$ are column vectors of length N = number of nodes, with entries:

$$h_\mu = \int_\Omega N_\mu h(T(\mathbf{x},t))\,d\Omega \quad \text{(nodal enthalpies)} \tag{43}$$

$$f_\mu = -\int_\Omega \nabla N_\mu\cdot k\nabla T(\mathbf{x},t)\,d\Omega$$

(nodal conductive fluxes) (44)

$$g_\mu = \int_\Omega N_\mu Q(\mathbf{x})\,d\Omega + \int_{\Gamma_q} N_\mu\bar{q}\,dS$$

(nodal external thermal loads). (45)

The difficulty comes from the fact that the relation between $\mathbf{T}$ and $\mathbf{h}$ is not one-to-one. The ODE's system is discretized in time according to a generalized trapezoidal rule as:

$$\frac{1}{\Delta t}(\mathbf{h}(\mathbf{T}(t+\Delta t)) - \mathbf{h}(\mathbf{T}(t))) = \alpha\mathbf{f}(\mathbf{T}(t+\Delta t)) + (1-\alpha)\mathbf{f}(\mathbf{T}(t)) + \mathbf{g}(t+\alpha\Delta t). \tag{46}$$

This scheme reduces to: forward Euler, Crank–Nicholson, Galerkin and backward Euler for $\alpha = 0$, 1/2, 2/3 and 1, respectively. For a given temperature vector $\mathbf{T}$ at time t, equation (46) is a nonlinear equation for $\mathbf{T}(t+\Delta t)$. Nonlinearity comes from the dependence of k and ρc_{p} on temperature and also from the change of phase which, as a matter of fact, could be viewed as a δ-type singularity in the $\rho c_{\text{p}}(T)$ relationship. The expression for the nodal enthalpies, equation (43), involves the integral over the element of the enthalpy

which is discontinuous at the interface. This integral must be evaluated very carefully, mainly by a reason of conditioning of the nonlinear system more than by a reason of accuracy [11, 12]. For instance, the classical numerical quadrature by Gauss points, so familiar in the FEM, gives nodal enthalpies with jumps at those nodal temperatures where the interface passes through a Gauss point.

For the implicit schemes ($\alpha \geqslant 1/2$), the nonlinear system is solved by Newton–Raphson iteration, and a correct evaluation of the Jacobian is the key feature to obtain good convergence properties. Besides the usual terms in the Jacobian, like the conductivity matrix and the capacity matrix corresponding to sensible heat, there is a term coming from the latent heat which dominates at small Stefan numbers (high latent heat), and whose expression is [12]:

$$M^{\mathrm{L}}_{\mu\nu} = \frac{\partial h^{\mathrm{L}}_{\mu}}{\partial T_{\nu}} = \int_{T=T_{\mathrm{m}}} N_{\mu}(\mathbf{x}) \frac{L}{|\nabla T|} N_{\nu}(\mathbf{x})\, \mathrm{d}S \qquad (47)$$

where h^{L} is that part of the enthalpy coming from the latent heat. The integral is calculated over the interface $T = T_{\mathrm{m}}$, and its physical significance shows up if the factor $L/|\nabla T|$ is interpreted as the specific heat per unit area of the interface. In numerical experiments at low Stefan numbers (high latent heat) the full Newton–Raphson method has been proved to be much more efficient and robust than secant methods, i.e. methods which do not include this interface capacity matrix.

There is a point to be clarified regarding the character of the thermal load vector coming from the heat source $Q(\mathbf{x}, t)$. In fact, this is not a standard heat source since it depends on the temperature vector through the position of the interface, besides the explicit dependence of the flux density on the temperature of the ablating surface. Then, it contributes also with a term to the Jacobian of the system, whose expression is rather complicated: it has one term coming from a change in the interpolation function at the interface due to its movement and another coming from a change in the curvature of the interface [13]. We have not included this term in the iteration matrix, but no instability has been observed, as it could be expected.

5. NUMERICAL EXAMPLES

5.1. *One-dimensional example with exact solution by truncation of the Neumann solution*

5.1.1. *Problem description.* Consider the following standard unsteady heat-conduction problem with constant coefficients in a semi-infinite medium:

$$\rho c_{\mathrm{p}} \dot{T} = k \frac{\partial^2 T}{\partial x^2} \quad \text{for } x > 0, t > 0$$

$$T(0, t) = T_{\mathrm{w}}$$

$$T(x, 0) = T_{\mathrm{i}}. \qquad (48)$$

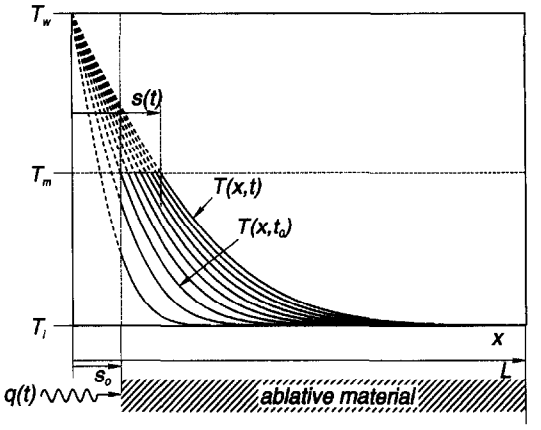

Fig. 6. 1D problem with exact solution. Problem description.

with $T_{\mathrm{i}} < T_{\mathrm{w}}$ (see Fig. 6). The so-called Neumann solution is obtained by similarity arguments in terms of the error function:

$$T(x, t) = T_{\mathrm{w}} - (T_{\mathrm{w}} - T_{\mathrm{i}}) \operatorname{erf}\left(\frac{x}{\sqrt{4Dt}}\right) \qquad (49)$$

where $D = k/\rho c_{\mathrm{p}}[=]\mathrm{m}^2\ \mathrm{s}^{-1}$ is the diffusivity, and the error function is defined as:

$$\operatorname{erf}(x) = \frac{2}{\sqrt{\pi}} \int_0^x \mathrm{e}^{-x'^2}\, \mathrm{d}x'$$

$$\operatorname{erf}(0) = 0 \quad \operatorname{erf}(+\infty) = 1. \qquad (50)$$

The ablation problem is constructed choosing some phase-change temperature T_{m}, $T_{\mathrm{i}} < T_{\mathrm{m}} < T_{\mathrm{w}}$, a latent heat $L > 0$ and an arbitrarily chosen initial surface position $s_0 > 0$, and selecting the heat flux history $\bar{q}(t)$ such that the resulting temperature field is given by (49) (see Fig. 6).

The position of the interface is obtained from:

$$T(s(t), t) = T_{\mathrm{m}} \qquad (51)$$

$$\frac{s(t)}{\sqrt{4Dt}} = \operatorname{erf}^{-1}\left(\frac{T_{\mathrm{w}} - T_{\mathrm{m}}}{T_{\mathrm{w}} - T_{\mathrm{i}}}\right) = s^* \quad \dot{s} = s^* \sqrt{\frac{D}{t}} \qquad (52)$$

and, the preheating time t_0 is given by:

$$\frac{s_0}{\sqrt{4Dt_0}} = s^*. \qquad (53)$$

For $t < t_0$ the heat to be applied at s_0 is given by:

$$\bar{q}(t) = -k \left.\frac{\partial T}{\partial x}\right|_{s_0} \quad t < t_0 \qquad (54)$$

and for $t > t_0$ the latent heat delivered must be taken into account:

$$\bar{q}(t) = L\dot{s} - k \left.\frac{\partial T}{\partial x}\right|_{s(t)^+} \quad t > t_0. \qquad (55)$$

Replacing the expression for the temperature field from equation (49) and the recession rate from equa-

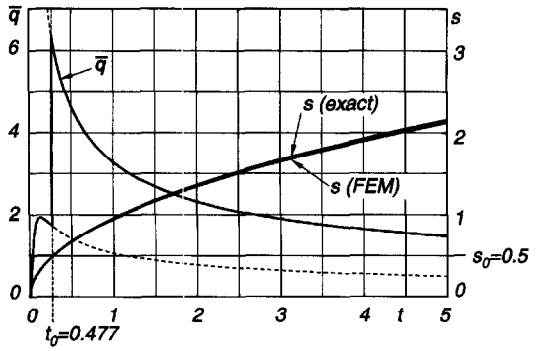

Fig. 7. 1D problem with exact solution. Time dependence of the thermal load, and the position of the ablating surface $s(t)$.

tion (52), the explicit expression for the thermal load is:

$$\bar{q}(t) = \begin{cases} \dfrac{2}{\sqrt{\pi}}\dfrac{k}{\sqrt{4Dt}}(T_w - T_i)\exp\left(-\dfrac{s_0^2}{4Dt}\right) & \text{for } t < t_0 \\ \dfrac{1}{\sqrt{4Dt}}\left(2Ls^*D + \dfrac{2}{\sqrt{\pi}}k(T_w - T_i)\,e^{-s^{*2}}\right) & \text{for } t > t_0 \end{cases} \tag{56}$$

(see Fig. 7). The thermal load is discontinuous at $t = t_0$, and the magnitude of the jump is:

$$\bar{q}(t_0 + 0) - \bar{q}(t_0 - 0) = \frac{2Ls^*D}{\sqrt{4Dt_0}}. \tag{57}$$

5.1.2. *Numerical results.* The problem was solved numerically for the following values:

$$T_w = 2 \quad T_m = 1 \quad T_i = 0$$

$$\rho c_p = k = 1 \quad L = 5 \quad s_0 = 0.5$$

from which:

$$Ste = \frac{\rho c_p (T_m - T_i)}{L} = 0.2 \quad D = 1$$

$$s^* = 0.477 \quad t_0 = 0.275.$$

The heat flux history is (see Fig. 7):

$$\bar{q}(t) = \begin{cases} \dfrac{1.128}{\sqrt{t}}e^{-0.0625/t} & t < 0.275 \\ \dfrac{3.283}{\sqrt{t}} & t > 0.275 \end{cases}.$$

The interval $0.5 \leqslant x \leqslant 7$ has been discretized with 50 elements with a non-uniform mesh size such that the size of the first element is one-tenth the size of the last one.

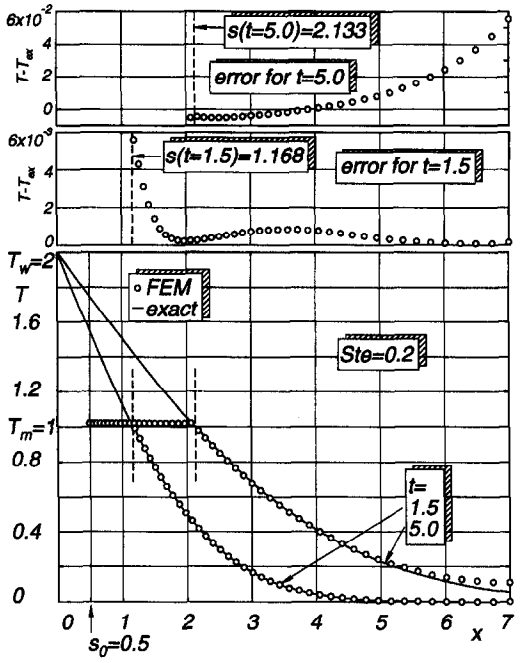

Fig. 8. Comparison between exact and numerical solutions at $t = 1.5$ and 5.

In Fig. 8, we compare the numerical solution and the exact one for $t = 1.5$ and $t = 5$, and in both cases they agree very well, showing at the top the nodal error for both time levels. For $t = 5$ there is a significant difference near the right ($x = 7$) boundary due to the fact that temperatures are already significant there. This causes a 'reflection' at the artificial boundary which is not present in the analytical solution. The fact that the discrete solution is almost equal to twice the analytical solution confirms this assertion. Finally, the temperature profile in the fictitious phase is not exactly T_m, but a little higher. This phenomenon will be explained for the constant load case in Section 5.2.1. The position of the ablating surface is compared against the exact one in Fig. 7.

5.2. *Asymptotic solution for the constant load problem*

5.2.1. *Problem description.* Let us consider now the typical case of a semi-infinite ($x > 0$) constant-coefficients problem with a constant heat load $\bar{q} \neq \bar{q}(t)$. For $t \to \infty$ the solution approaches asymptotically a steady profile moving at constant speed:

$$\dot{s} \to v_\infty \quad T(x,t) = f(x - s(t))(T_m - T_i) + T_m \tag{58}$$

where v_∞ is the limit recession rate and f is the normalized profile satisfying $f(0) = 0$ and $f(\infty) = 1$. As is typical in thermal transients, the approach to the limit solution is exponential, and we can put:

$$s(t) = -s_\infty + v_\infty t + O(e^{-t/\tau}) \tag{59}$$

where s_∞ is a limit shift produced by the transient and τ a characteristic decay time. v_∞ is easily obtained from a power balance:

$$(L+\rho c_p(T_m-T_i))v_\infty = \bar{q}. \quad (60)$$

Replacing equation (58) in the heat conduction equation, and changing to a coordinate system attached to the moving profile, a simple ODE for f is obtained, whose solution is an exponential function. The resulting temperature profile is:

$$T(x,t) = T_m-(T_m-T_i)\left\{1-\exp\left(-\frac{x-v_\infty t+s_\infty}{l}\right)\right\}$$

$$\text{for } x > v_\infty t - s_\infty \quad (61)$$

where the characteristic decay length of the profile in the medium is: $l = D/v_\infty$. Finally, the limit shift is obtained from a balance of the total energy applied to the body:

$$\bar{q}t = [L+\rho c_p(T_m-T_i)](v_\infty t - s_\infty) + \rho c_p(T_m-T_i)l\int_0^\infty e^{-\xi}\,d\xi \quad (62)$$

and results in:

$$s_\infty = \frac{l}{1+Ste^{-1}}. \quad (63)$$

This asymptotic solution is known as the "evaporation-controlled limit".

It is interesting to see that a similar "steady solution" exists for the proposed scheme, exhibiting exact asymptotic velocity, i.e. a solution that behaves (for $t\to\infty$) as a steadily propagating temperature profile:

$$T^{n+1}(x) = T^n(x-\Delta s). \quad (64)$$

Moerover, due to the energy conserving property of the enthalpy formulation $\Delta s = v_\infty \Delta t$, i.e. the asymptotic velocity is obtained exactly by the discrete scheme. For simplicity we will describe it for the case when the discretization is performed in time only, and later we will see through the examples that this property is found in the fully discretized version.

The 1D version of equation (28) for constant properties, discretized in time with a two-step backward Euler scheme is:

$$\frac{h(T^{n+1})-h(T^n)}{\Delta t} = -k\frac{\partial^2 T^{n+1}}{\partial x^2} + \bar{q}\delta(s^n). \quad (65)$$

Note that the external heat load is taken into account explicitly. Replacing equation (64) in (65) and integrating from $x=0$ to ∞ it is shown that:

$$\frac{\Delta s}{\Delta t} = v_\infty. \quad (66)$$

Assuming $T_i = 0$ for simplicity, the equations governing the steady state discrete solution are:

$$\rho c_p\frac{T^{n+1}-T^n}{\Delta t} = -k\frac{\partial^2 T^{n+1}}{\partial x^2} \quad \text{in } x > s^{n+1} \quad (67)$$

$$\frac{\rho c_p T_m + L - \rho c_p T^n}{\Delta t} = -k\frac{\partial^2 T^{n+1}}{\partial x^2} \quad \text{in } s^n < x < s^{n+1} \quad (68)$$

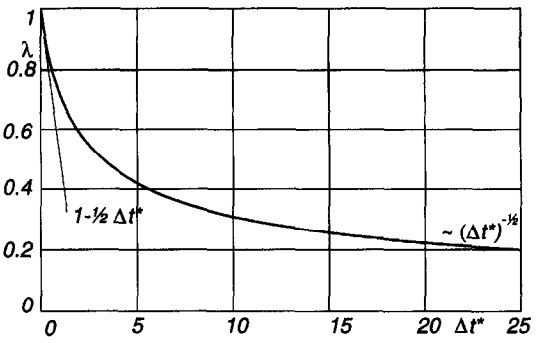

Fig. 9. Dependence of the correction factor λ for the characteristic decay length of the discrete solution versus the non-dimensional time-step Δt.

$$\frac{\partial T^{n+1}}{\partial x^2} = 0 \quad \text{in } x < s^n \quad (69)$$

with the following matching conditions:

$$0 = -k\left.\frac{\partial T^{n+1}}{\partial x}\right|_{(s^{n+1})+} + k\left.\frac{\partial T^{n+1}}{\partial x}\right|_{(s^{n+1})-} \quad \text{at } x = s^{n+1} \quad (70)$$

$$\bar{q} = -k\left.\frac{\partial T^{n+1}}{\partial x}\right|_{(s^n)+} + k\left.\frac{\partial T^{n+1}}{\partial x}\right|_{(s^n)-} \quad \text{at } x = s^n. \quad (71)$$

We refer to the region $s^n \leqslant x \leqslant s^{n+1}$ as the "transition region", i.e. the region that is being ablated in the current time step. The solution to equations (67)–(71) can be found as [13]:

$$T^{n+1} = \begin{cases} T_m\theta(1) & \text{for } x \leqslant s^n \\ T_m\theta(\mu) & \text{for } s^n \leqslant x \leqslant s^{n+1} \\ T_m \exp\left(-\dfrac{\lambda(x-s^{n+1})}{l}\right) & \text{for } x \geqslant s^{n+1} \end{cases} \quad (72)$$

where $\theta = T/T_m$ and $\mu = (s^{n+1}-x)/\Delta s$ are the non-dimensional temperature and spatial coordinate in the transition region:

$$\theta(\mu) = \left\{1+\lambda\Delta t^* + \Delta t^*(1+Ste^{-1})\frac{\mu^2}{2} + \frac{e^{-\lambda\Delta t^*}}{\lambda}\left(\mu - \frac{e^{\lambda\Delta t^*\mu}-1}{\lambda\Delta t^*}\right)\right\} \quad (73)$$

$\Delta t^* = \Delta t v_\infty^2/D$ is the non-dimensional time step and l/λ is the characteristic decay length for the discrete problem (65), satisfying the transcendental equation:

$$\frac{1-e^{-\lambda\Delta t^*}}{\lambda\Delta t^*} = \lambda \quad (74)$$

(see Fig. 9). As $\lambda < 1$, the temperature in the fictitious

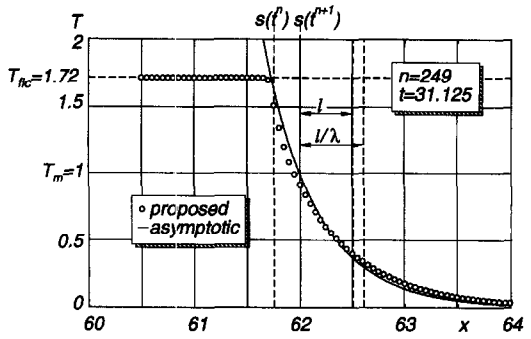

Fig. 10. Comparison of proposed FEM and asymptotic solutions for the constant load problem.

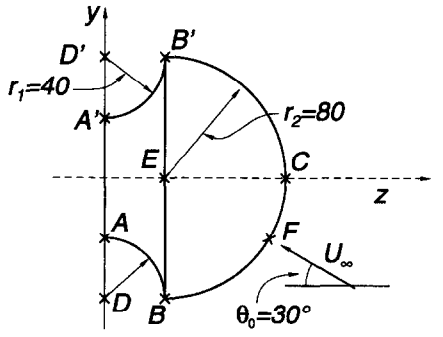

Fig. 11. Geometry description for the 3D problem. (All dimensions in mm.)

phase, other than the transition region, $x < s^n$ is always greater than the melting temperature:

$$T_{\text{fic}} = T_{\text{m}}\left\{1+1/2\Delta t^*(1+Ste^{-1})+\frac{1}{\lambda}-1\right\} \geqslant T_{\text{m}}. \tag{75}$$

With respect to the precision of the scheme, the error in the position of the ablating surface is, asymptotically:

$$s^n - s(n\Delta t) = -\frac{Ste}{Ste+1}\left(\frac{1}{\lambda}-1\right)l \tag{76}$$

so that the position of the discrete ablating surface is always retarded with respect to the exact one. As $\lambda \to 1$ for $\Delta t^* \to 0$ it can be shown that $T_{\text{fic}} \to T_{\text{m}}$, $s^n \to s(n\Delta t)$ and $l/\lambda \to l$, so that the discrete profile converges to the exact one.

5.2.2. *Numerical results.* The problem has been solved for the following physical data:

$$T_{\text{m}} = 1 \quad \rho c_{\text{p}} = k = D = 1 \quad L = 1 \quad \bar{q} = 4.$$

For the discretization, we have taken $\Delta t = 0.125$ and a uniform mesh with $\Delta x = 0.05$. To assure that the asymptotic solution is reached the simulation has been followed for a very long period of time $t = 32$, what is more than 120 times the characteristic decaying time $\tau = l/v_\infty = 0.25$. Such a simulation would required a mesh of length $v_\infty t = 64$, at least, what is equivalent to 64/0.05 = 1280 elements. Instead we performed all the simulation in a mesh of length 10 (200 elements), by partitioning the entire simulation in 32 small subperiods $\Delta t_{\text{sp}} = 1$. At the end of each sub-period the entire profile was displaced by a length $\Delta s_{\text{sp}} = v_\infty \Delta t_{\text{sp}}$. In Fig. 10 we can see the computed temperature profile and the asymptotic one. The temperature in the fictitious zone is $T_{\text{fic}} = 1.72$ and the error in the ablating surface position is $s^n - s(n\Delta t) = 0.0548$ in perfect agreement with the prediction from equations (75) and (76). The position of the ablating surface s^n is evaluated by computing the intersection of the linear temperature profile in the element with the ablating temperature. From this, an approximation for the recession rate $\dot{s}^{n+1/2} = (s^{n+1} - s^n)/\Delta t$ is obtained. This value was exact to eight digits. This behavior is possible only if the length traversed by the ablating surface asymptotically Δs is equal to an integer number of elements. In this case $\Delta s = 0.25 = 5\Delta x$. If this is not the case, but $\Delta s/\Delta x = p/q$ with p, q integers then the averaged velocity over q consecutive time steps is exact. We checked this by performing a numerical experiment similar to the previous one but with a $\Delta t = 0.0625$, i.e. one half the previous one. The ablating surface travels asymptotically 2.5 elements each time step. The computed recession rates oscillates between the following two values: $\dot{s}^{2n-1/2} = 2.0034072$, $\dot{s}^{2n+1/2} = 1.9965927$, giving an averaged velocity correct to eight digits again.

5.3. *Ablation of a thermal protection*

5.3.1. *Problem description.* The geometry can be observed in Fig. 11 and consists of a solid of revolution whose intersection with the meridian plane $x = 0$ is shown. For the physical properties we use those ones representative of virgin silica phenolic (see Table 1): pyrolysis is taken into account as a phase-change at a fixed temperature of $T_{\text{p}} = 800$ K and ablation occurs at a fixed temperature of $T_{\text{m}} = 2666$ K.

The boundary conditions are: adiabatic at the toroidal section $AB-A'B'$ and at the rear plane AA'. A thermal load arising from aerodynamic heating at an incidence of 30° on the $x = 0$ plane is applied to the spheric surface $B'CB$. The thermal load is constant in time for $t > 0$ and depends on position as:

$$\bar{q}(P) = \bar{q}_0 \cos\beta$$
$$= \bar{q}_0(\cos\theta\cos\theta_0 - \sin\theta\sin\theta_0\sin\varphi)$$

with $\bar{q}_0 = 0.04$ kW/cm^2 and θ, φ are spherical coordinates with respect to the center E of a generic point P on the spherical surface:

$$z = z_{\text{E}} + r_2\cos\theta$$
$$x = r_2\sin\theta\cos\varphi$$
$$y = r_2\sin\theta\sin\varphi.$$

β is the angle between the segments EP and EF with F the stagnation point (maximum heat load density) at $\varphi = -90°$ and $\theta = \theta_0 = 30°$. This thermal load is proposed only in order to test the model and does not

Table 1. Physical properties for the 3D numerical example

Phase	ρ [kg m^{-3}]	k [kW m^{-1} K^{-1}]	c_p [kJ kg^{-1} K^{-1}]	Transition
$(\ )_v$	1656	0.69×10^{-3}	1.26	Pyrolysis, $T_p = 800$ K
$(\ )_c$	1324	1.04×10^{-3}	1.05	Ablation, $T_m = 2666$ K

take into account the coupling between the shape and the aerodynamic heating on a re-entry vehicle.

Initially, the body is at a uniform temperature of $T_i = 300$ K. The limit recession rate (for a 1D equivalent problem) is:

$$v_\infty = \frac{\bar{q}_0}{\rho_v c_{p_v}(T_p - T_i) + (\rho L)_p + \rho_c c_{p_c}(T_m - T_p) + \rho_c L_m}$$
$$= 4.47\times10^{-3}\ \text{cm s}^{-1}$$

and the typical decaying length of the normal temperature profile is $l = 1.67$ cm.

5.3.2. *Numerical modeling.* Only the $x > 0$ half of the problem was modeled by symmetry. The FEM mesh is shown in Fig. 12 and has 5061 nodes and 4320 elements. Note that it is highly refined near the external surface, in the normal direction.

The first proposed method was used, i.e. imposing the thermal load always at the external surface, since the CPU-time requirements for this method is usually smaller. Recall that, in fact, this method ceases to be valid if large variations of the thermal load on the surface are present, but this is not the case for this problem. The temporal evolution was followed up to $t = 500$ s with 50 time steps of $\Delta t = 10$ s.

5.3.3. *Numerical results.* We show in Fig. 13 the temperature profiles on the intersection of the plane of symmetry $x = 0$ and the external surface. The ablation

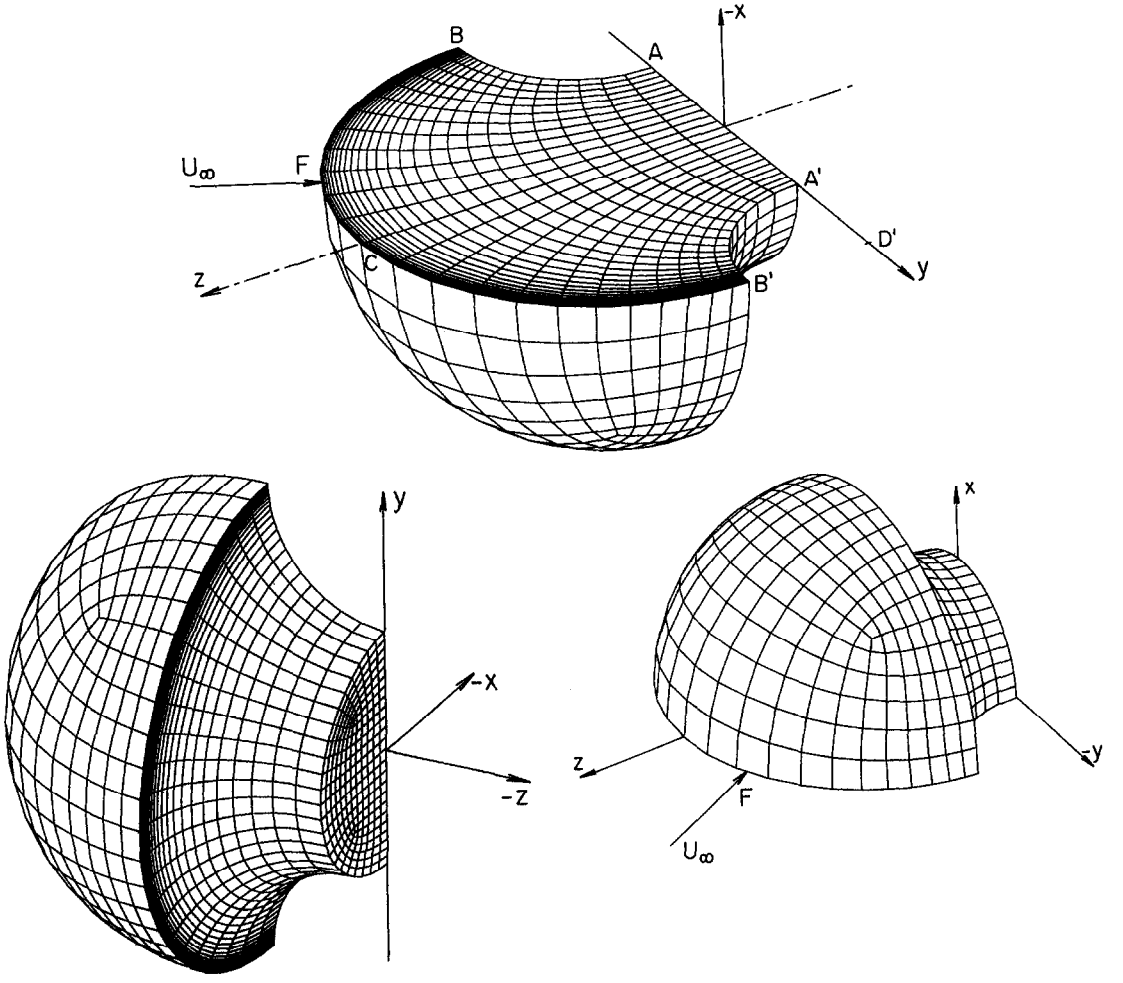

Fig. 12. 3D FEM-mesh view.

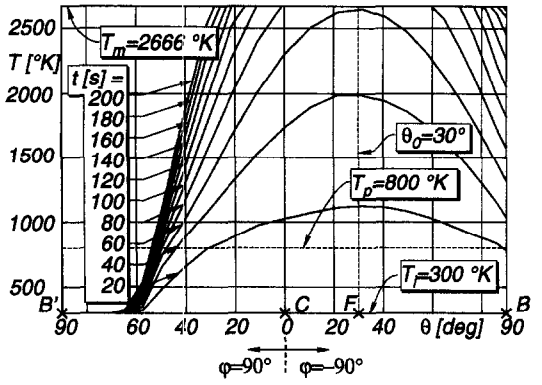

Fig. 13. Temperature profiles at the intersection of the $x = 0$ plane with the external spherical surface.

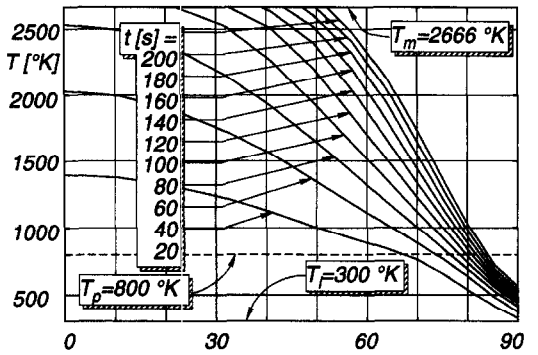

Fig. 14. Temperature profiles at the intersection of the $y = 0$ plane with the external spherical surface.

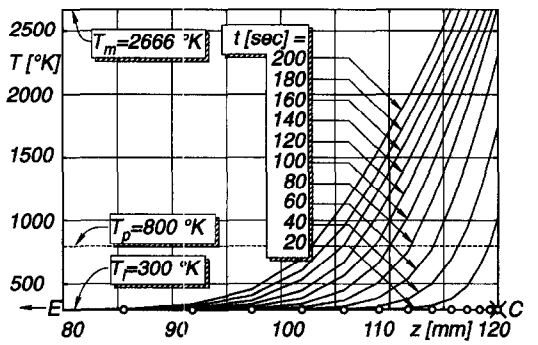

Fig. 15. Temperature profiles at z-axis.

temperature is reached at $t \approx 50$ s. In Fig. 14 we see the temperature profiles on the plane $y = 0$, and in Fig. 15 those on the z-axis. In this last figure we also show the location of nodes on the z-axis as small circles. Finally, we can see in Fig. 16 the shape progression for $t = 100$, 200 and 300 s. The run was performed on an Intel i486/50MHz based personal computer.

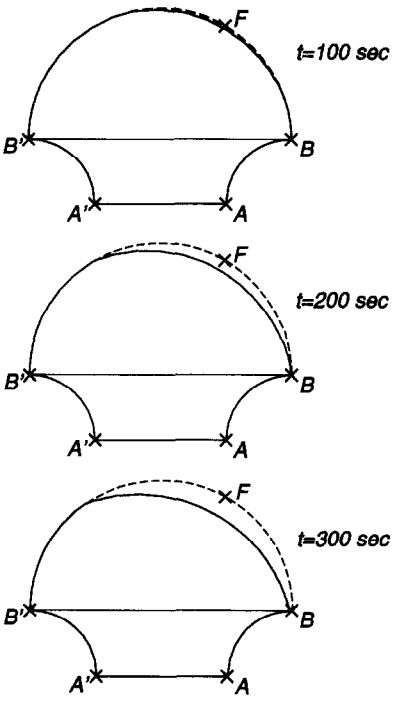

Fig. 16. Shape progression.

6. CONCLUSIONS

An equivalent two-phase formulation is presented, which allows the modeling of ablation problems by means of a robust solver for the two-phase problem. The removed part is replaced by a fictitious material with null specific heat and the thermal load at the interface is added as a strongly localized heat source. The recession rate is predicted exactly for the 1D constant-load problem. The temperature in the fictitious phase is almost constant, higher than the melting temperature. Future work will be concentrated mainly in the extension to non-isothermal ablation and in implementing some kind of local refinement at the ablating surface in order to correctly model the jump in temperature gradient there.

Acknowledgement—The author wishes to express his gratitude to Consejo Nacional de Investigaciones Científicas y Técnicas (CONICET, Argentina) for its financial support.

REFERENCES

1. M. Hogge and P. Gerrekens, Two-dimensional deforming finite element methods for surface ablation, *AIAA J.* **23**, 465–472 (1982).
2. P. Gerrekens, Modelisation par elements finis des phenómenes d'ablation thermique avec pyrolise, Ph. D. Thesis, Liège University, Belgium (1987).
3. T. Cai and X. Hou, A simple method for tackling moving boundary in numerical simulation of temperature response of the solid rocket motor, AIAA paper 88-0083 (1988).
4. K. K. Muramoto, T. H. Squire and C. F. Thompson,

Jr., A thermal analysis code for three-dimensional wing leading edges, AIAA Paper 91-1354, (1991).
5. B. F. Blackwell and R. E. Hogan, One-dimensional ablation using Landau transformation and finite control volume procedure, *J. Thermophys. Heat Transfer* **8,** 282–287 (1994).
6. W. L. Hunter and J. R. Kuttler, Enthalpy method for ablation-type moving boundary problems, *J. Thermophys.* **5,** 240–242 (1991).
7. K. H. Tacke, Discretization of the explicit enthalpy method for planar phase change, *Int. J. Numer. Meth. Engng* **21,** 543–554 (1985).
8. K. K. Tamma and R. Namburu, Recent advances, trends and new perspectives via enthalpy-based finite element formulations for applications to solidification problems, *Int. J. Numer. Meth. Engng* **30,** 803–820 (1990).
9. Q. T. Pham, The use of lumped capacitance in the finite-element solution of heat conduction problems with phase change, *Int. J. Heat Mass Transfer* **29,** 285–291 (1986).
10. V. Voller and M. Cross, Accurate solutions of moving boundary problems using the enthalpy methods, *Int. J. Heat Mass Transfer* **24,** 545–556 (1981).
11. M. A. Storti, L. A. Crivelli and S. R. Idelsohn, Making curved interfaces straight in phase-change problems, *Int. J. Numer. Meth. Engng* **24,** 375–392 (1987).
12. M. A. Storti, L. A. Crivelli and S. R. Idelsohn, An efficient tangent scheme for phase-change problems, *Computer Meth. Appl. Mech. Engng* **66,** 65–86 (1988).
13. M. A. Storti, Modeling ablation problems as two phase Stefan problems, GTM-INTEC 10/94, Santa Fe, Argentina (in Spanish).